Electronic Supplementary Material (ESI) for Analytical Methods.

Supplementary materials:

Dual-template imprinted polymer electrochemical sensor for simultaneous determination of malathion and carbendazim using graphene quantum dots

Fariba Beigmoradi[a], Masoud Rohani Moghadam*[,a], Zahra Garkani-Nejad[b], Alireza Bazmandegan-Shamili[a], Hamid Reza Masoodi[a]

[a] Department of Chemistry, Faculty of Sciences, Vali-e-Asr University of Rafsanjan, Rafsanjan, Iran.
[b] Department of Chemistry, Faculty of Sciences, Shahid Bahonar University of Kerman, Kerman, Iran.

***Correspondence**
Masoud Rohani Moghadam, Department of Chemistry, Faculty of Sciences, Vali-e-Asr University of Rafsanjan, Rafsanjan, Iran.

E-mail: masoud.rohani.moghadam@gmail.com; m.rohani@vru.ac.ir

How to perform computational calculations for the pH of the extraction

The environmental pH affects the stability of the MAL and CBZ. The protonated and deprotonated forms of MAL and CBZ can be created in alkaline and acidic media. MAL/CBZ and their several tautomers of deprotonated (MAL^-/CBZ^-) and protonated (MAL^+/CBZ^+) are shown in Fig. 7S† and Fig. 8S†, respectively. For this purpose, at first, the stability of neutral, deprotonated, and protonated forms of MAL and CBZ was studied using the binding energy (BE) by atom for any form matching to the following equation of S1† and S2†, respectively:

$$BE = \frac{\left[aE_C + bE_H + cE_{Cl} + dE_N + eE_O + fE_P + gE_S\right] - E}{a + b + c + d + e + f + g} \quad \text{eq. S1}$$

$$BE = \frac{\left[aE_C + bE_H + dE_N + eE_O\right] - E}{a + b + d + e} \quad \text{eq. S2}$$

According to equation 1, a, b, c, d, e, f, and g are the number of C, H, Cl, N, O, P, and S atoms, respectively. EC, EH, ECl, EN, EO, EP, and ES are the ground state total energies of C, H, Cl, V, O, P, and S, respectively. Also, according to equation 2, a, b, c, and d are the number of C, H, N, and O atoms, respectively. EC, EH, EN, and EO are the ground state total energies of C, H, N, and O, respectively, and E is the total energy of the studied form. As shown in Table S1†, the amount of energy of the neutral, deprotonated, and protonated forms of MAL and CBZ in water conforms with: CBZ^-(I) > CBZ^-(II) > CBZ > CBZ^+(I) > CBZ^+(II) > CBZ^+(III), and MAL^- > MAL > MAL^+(V) > MAL^+(IV) > MAL^+(VI) > MAL^+(VII) > MAL^+(II) > MAL^+(III) > MAL^+(I) as can be seen that the BE amount gains by going from acidic media to alkaline media. That is the meaning a linear relationship can be found between the stability of MAL and CBZ forms and the pH of the medium.

On the other hand, the MAL-MAA and CBZ-MAA complexes are organized via hydrogen bonding. As the stability of hydrogen-bonded complexes is generally symmetrical to the number of hydrogen bonds, the following calculations were studied on the two hydrogen-bonded complexes of MAL-MAA (Fig. 9S†) and CBZ-MAA (Fig. 10S†).

So here, the complexation energy was calculated by the following formula:

$$\Delta E = E_{complex} - E_{template} - E_{monomer}$$

$E_{complex}$ represents the energy of the monomer-template complex, $E_{template}$ the energy of the template and $E_{monomer}$ the energy of the monomer. Figure. 10S(C),† shows that the proton transfer procedure happen in CBZ^--MAA(I), CBZ^--MAA(V), and MAL^--MAA(I) complexes. As Table 2S† shows, the interaction energies were as CBZ-MAA(I) > CBZ-MAA(II) > CBZ-MAA(III), and MAL–MAA(II) > MAL–MAA(IV) > MAL–MAA(I) > MAL–MAA(III) > MAL–MAA(VI) > MAL–MAA(VII) > MAL–MAA(V) in neutral media, CBZ^--MAA(I) > CBZ^--MAA(II) > CBZ^--

MAA(III) > CBZ^--MAA(IV) > CBZ^--MAA(V), MAL^-–MAA(V) > MAL^-–MAA(VI) > MAL^-–MAA(I) > MAL^-–MAA(VII) > MAL^-–MAA(II) > MAL^-–MAA(IV), and MAL^-–MAA(III) in alkaline media, CBZ^+-MAA, and MAL^+–MAA(V) > MAL^+–MAA(VII) > MAL^+–MAA(VI) > MAL^+–MAA(IV) ≈ MAL^+–MAA(III)> MAL^+–MAA(I) > MAL^+–MAA(II). So, CBZ^--MAA(I), MAL^-–MAA(V) complexes were the most stable complexes in neutral, acidic, and alkaline media, respectively. A comparison between the ΔE amounts of these complexes shows that the orientation of molecules to interact together gains from acidic to alkaline media.

Table 1S. The binding energies (kJmol-1) of neutral, protonated and deprotonated forms of MAL and CBZ in water.

Monomers	**BE(kJmol^{-1})**
MAL	498.85
MAL^{-}	514.33
MAL^{+}(I)	474.73
MAL^{+}(II)	477.79
MAL^{+}(III)	477.65
MAL^{+}(IV)	479.37
MAL^{+}(V)	479.39
MAL^{+}(VI)	478.81
MAL^{+}(VII)	478.44
CBZ	470.66
CBZ^{-}(I)	495.03
CBZ^{-}(II)	494.77
CBZ^{+}(I)	444.45
CBZ^{+}(II)	439.62
CBZ^{+}(III)	433.89

Complex	ΔE (kJmol^{-1})
MAL–MAA(I)	-28.26
MAL–MAA(II)	-34.67
MAL–MAA(III)	-25.05
MAL–MAA(IV)	-10.81
MAL–MAA(V)	-17.34
MAL–MAA(VI)	-23.42
MAL–MAA(VII)	-22.88
MAL^{-}–MAA(I)	-51.69
MAL^{-}–MAA(II)	-33.18
MAL^{-}–MAA(III)	-26.85
MAL^{-}–MAA(IV)	-28.83
MAL^{-}–MAA(V)	-52.04
MAL^{-}–MAA(VI)	-51.83
MAL^{-}–MAA(VII)	-46.20
MAL^{+}–MAA(I)	-13.81
MAL^{+}–MAA(II)	-12.74
MAL^{+}–MAA(III)	-21.71
MAL^{+}–MAA(IV)	-21.71
MAL^{+}–MAA(V)	-32.15
MAL^{+}–MAA(VI)	-24.97
MAL^{+}–MAA(VII)	-31.38
CBZ–MAA(I)	-66.53
CBZ–MAA(II)	-52.15
CBZ–MAA(III)	-38.70
CBZ^{-}–MAA(I)	-77.45
CBZ^{-}–MAA(II)	-55.58
CBZ^{-}–MAA(III)	-54.04
CBZ^{-}–MAA(IV)	-52.70
CBZ^{-}–MAA(V)	-48.99
CBZ^{+}–MAA	-54.77

Table 2S. The complexation energies (kJmol^{-1}) of studied complexes.

Table 3S. The effect of interfering species in the simultaneous measurement of 1.00 μM MAL and 5.00 μM CBZ solution.

Pesticide	**MAL**		
	Tolerance level (μM)	**Variation in signal[a]**	**Tolerance level (μM) for CBZ**
DLM	1200	+9.43%	1600
FNT	900	+9.62%	800
DZN	2200	-9.57%	2500
CPF	1500	-8.59%	1600

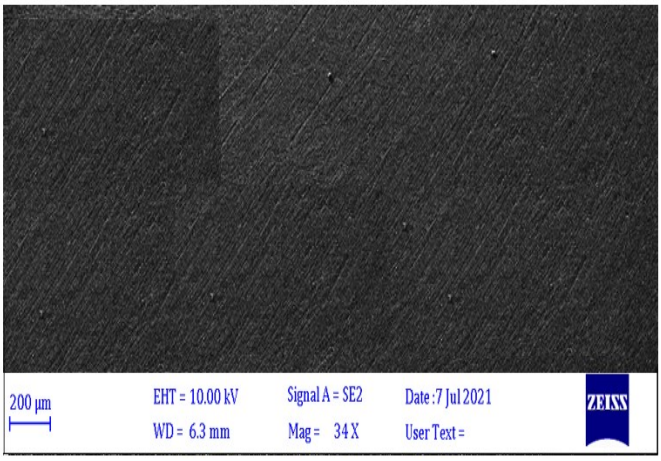

Figure 1S. FESEM image on the surface of polished GECE.

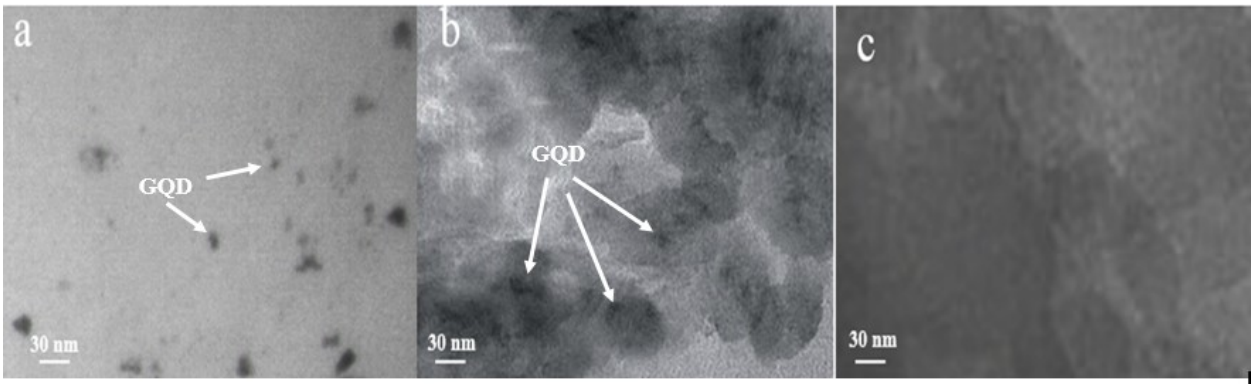

Figure 2S. TEM image of synthesized (a) GQDs, (b) GQDs@MIP, and (c) MIP.

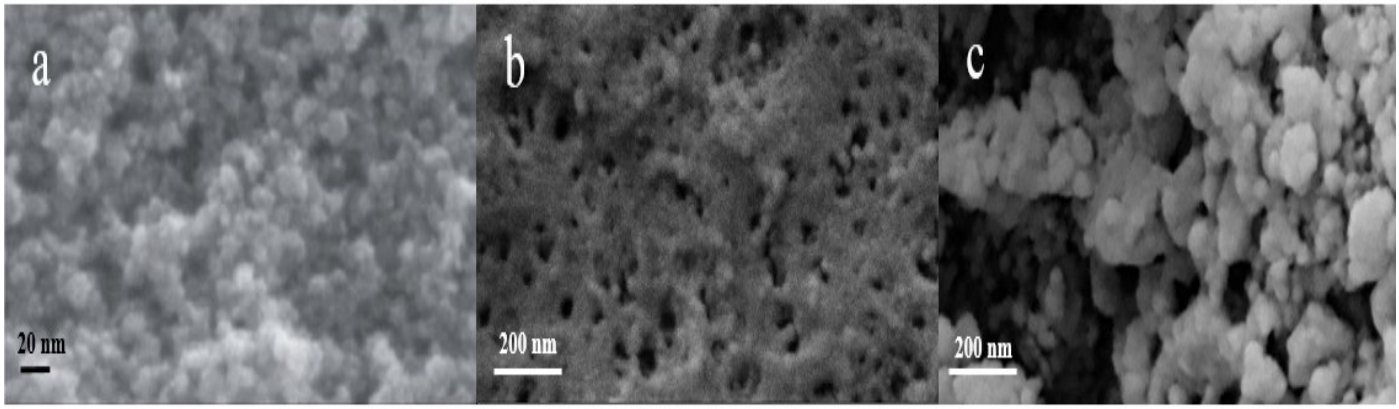

Figure 3S. FESEM images of the synthesized (a) GQDs, (b) MIP, and (c) GQDs@MIP.

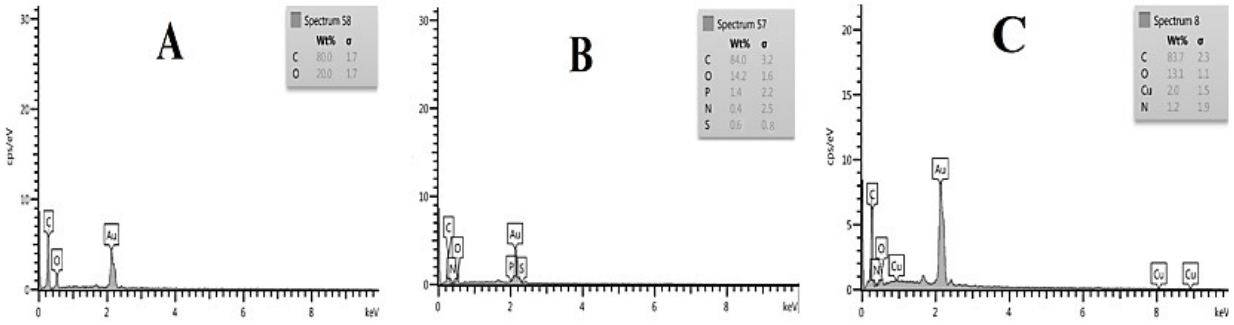

Figure 4S. EDS analysis of (A) GQDs, (B) GQDs@MIP (MAL), and (C) GQDs@MIP (CBZ).

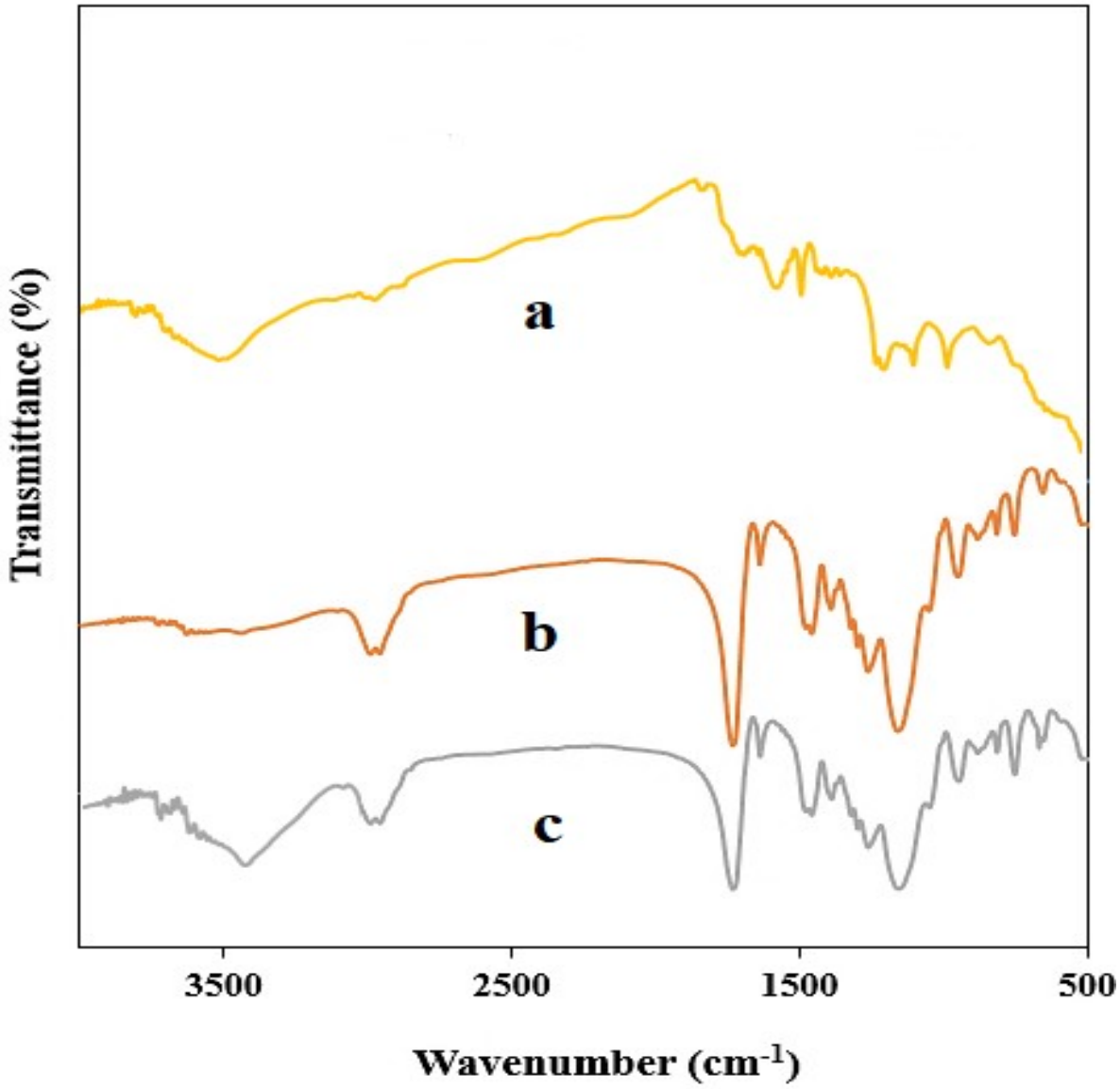

Figure 5S. FT-IR of (a) GQDs, (b) MIP, (c) GQDs@MIP.

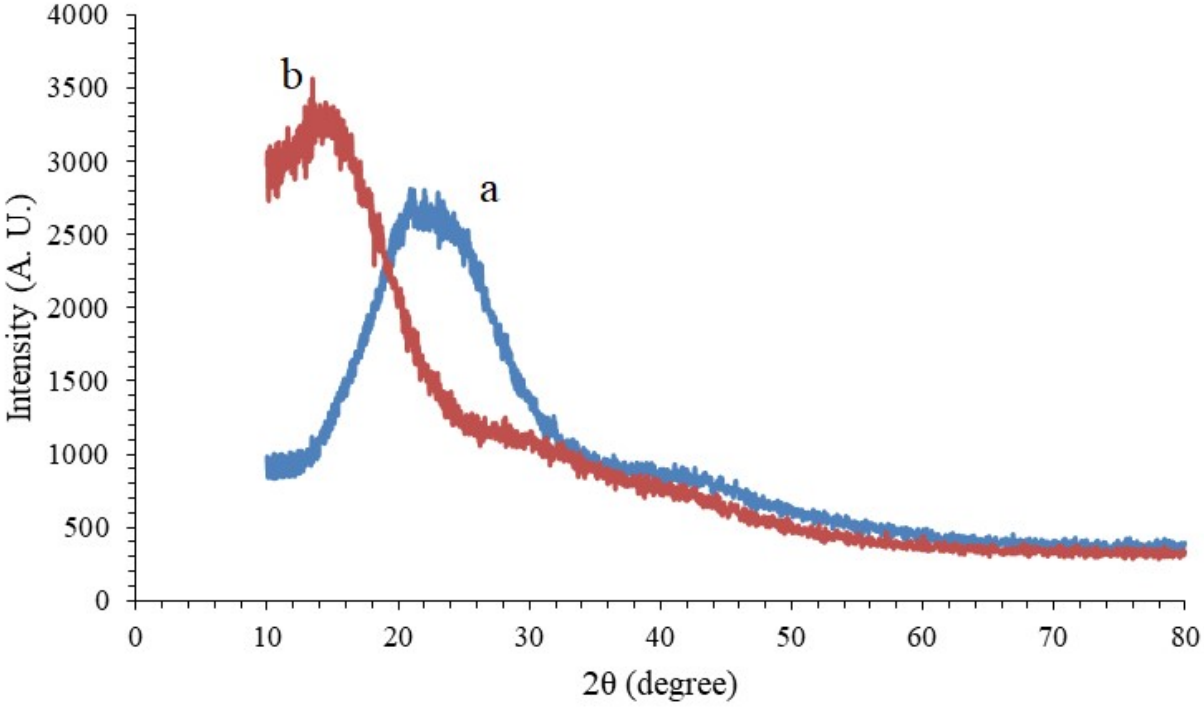

Figure 6S. XRD pattern of (a) GQDs and (b) GQDs@MIP.

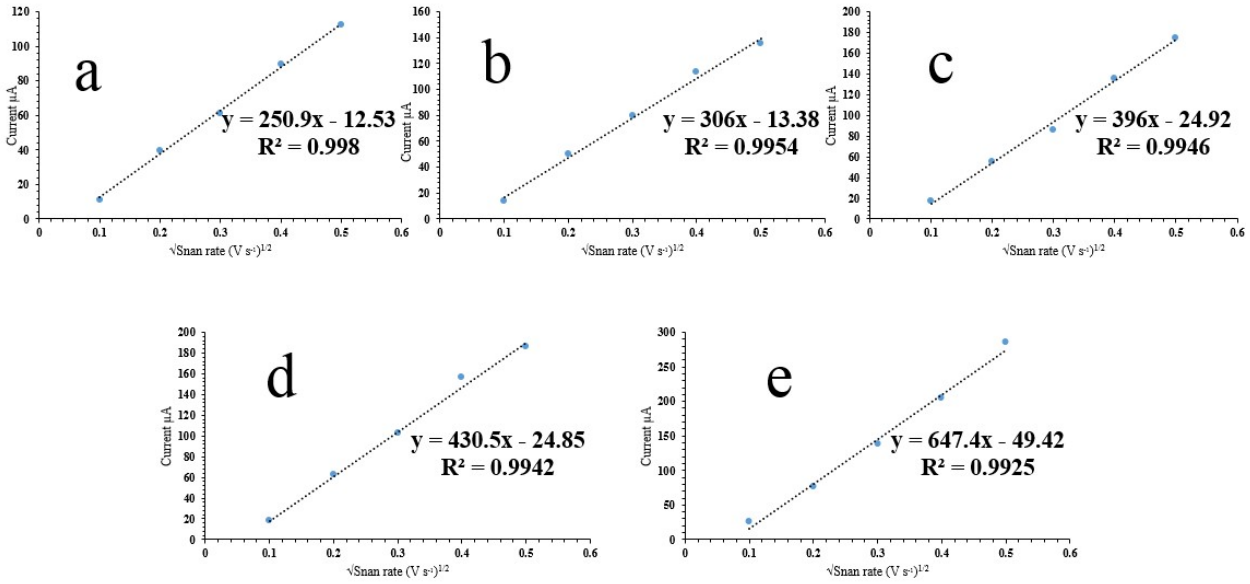

Figure 7S. Currents of CVs vs. square of scan rates for bare (a), GQD (b), NIP-GEC (c), MIP-GEC (d) and GQDs@MIP-GE (e) electrodes in 5 mM $Fe(CN)_6^{4-/3-}$ at different scan rates

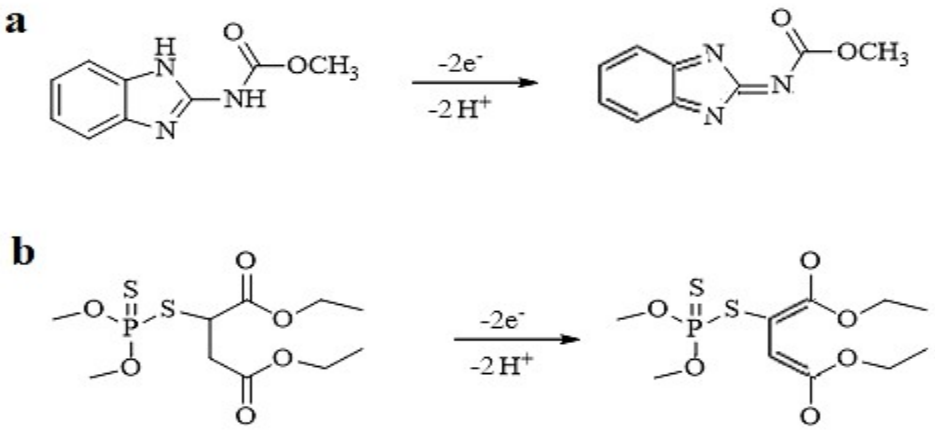

Figure 8S. (a) CBZ and (b) MAL oxidation mechanism.

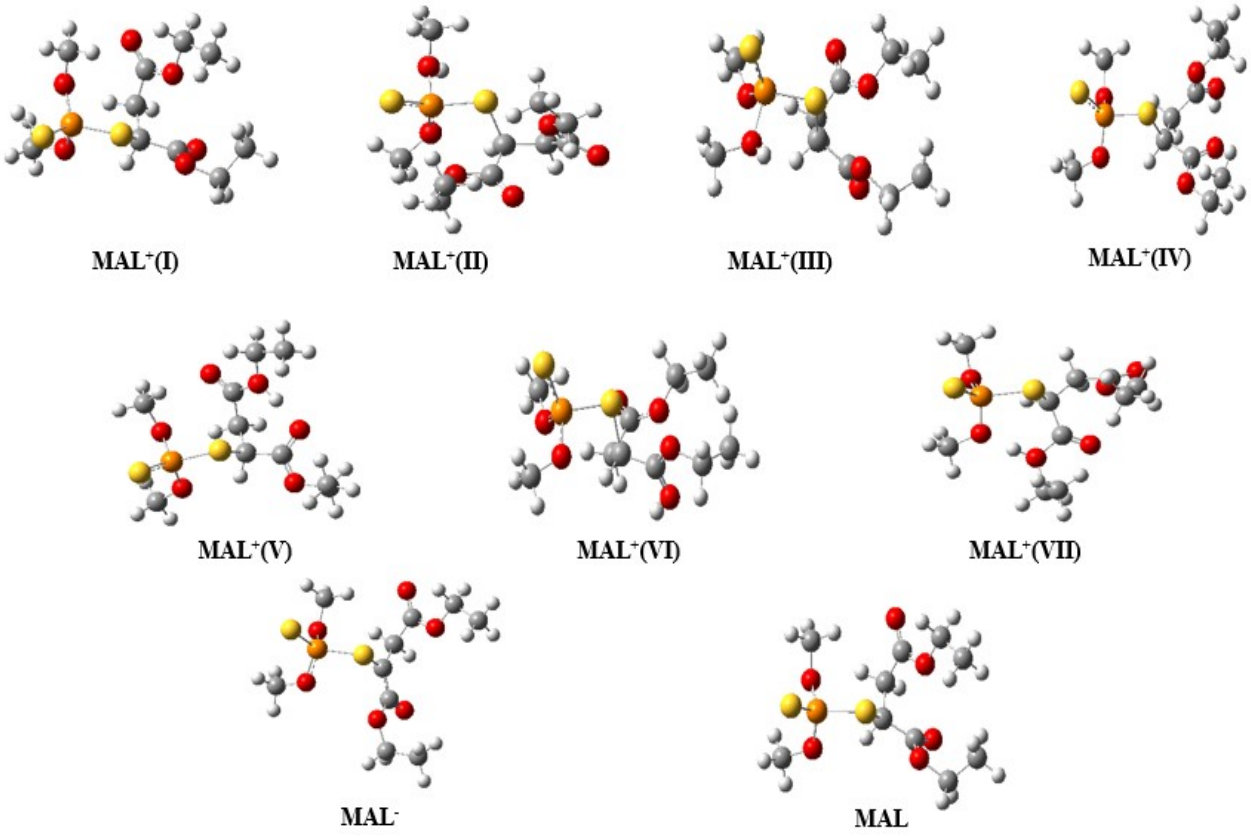

Figure 9S. The optimized structures of protonated, deprotonated, and neutral forms of MAL.

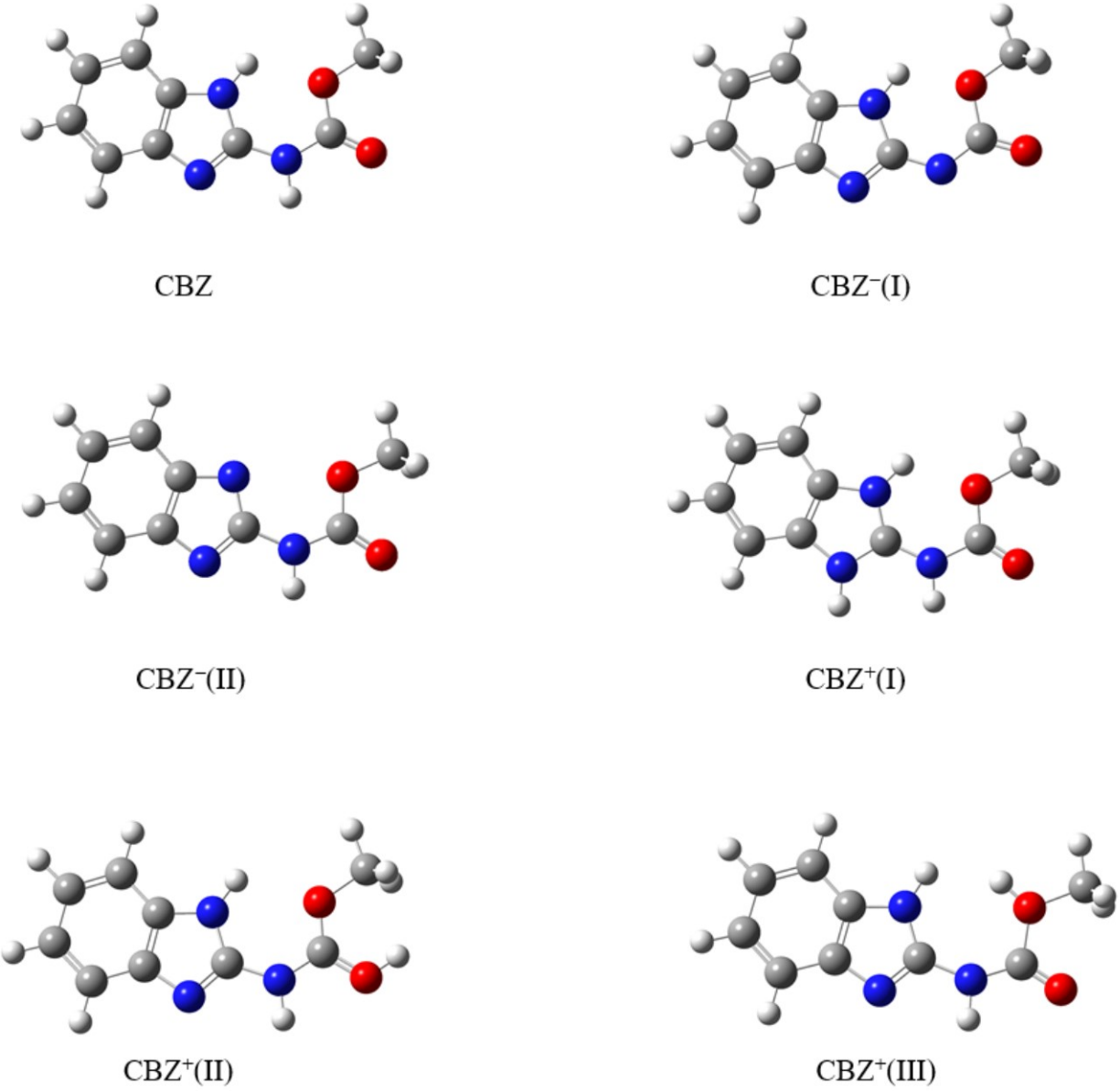

Figure 10S. The optimized structures of neutral, deprotonated, and protonated forms of CBZ.

A

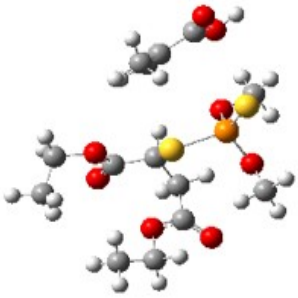

MAL-MAA(I)

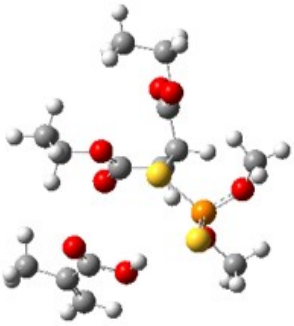

MAL-MAA(II)

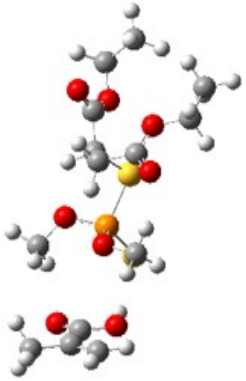

MAL-MAA(III)

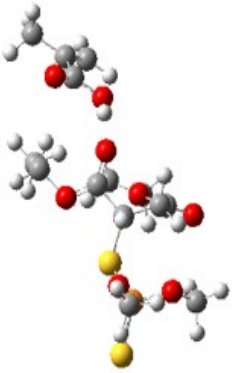

MAL-MAA(IV)

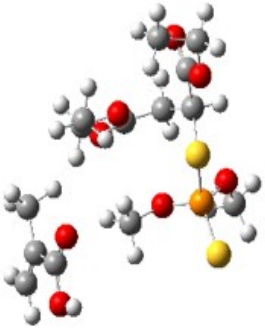

MAL-MAA(V)

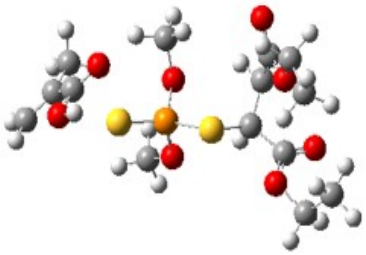

MAL-MAA(VI)

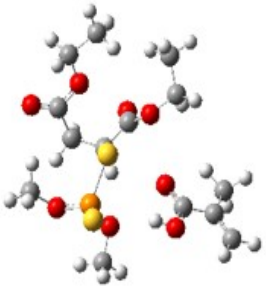

MAL-MAA(VII)

B

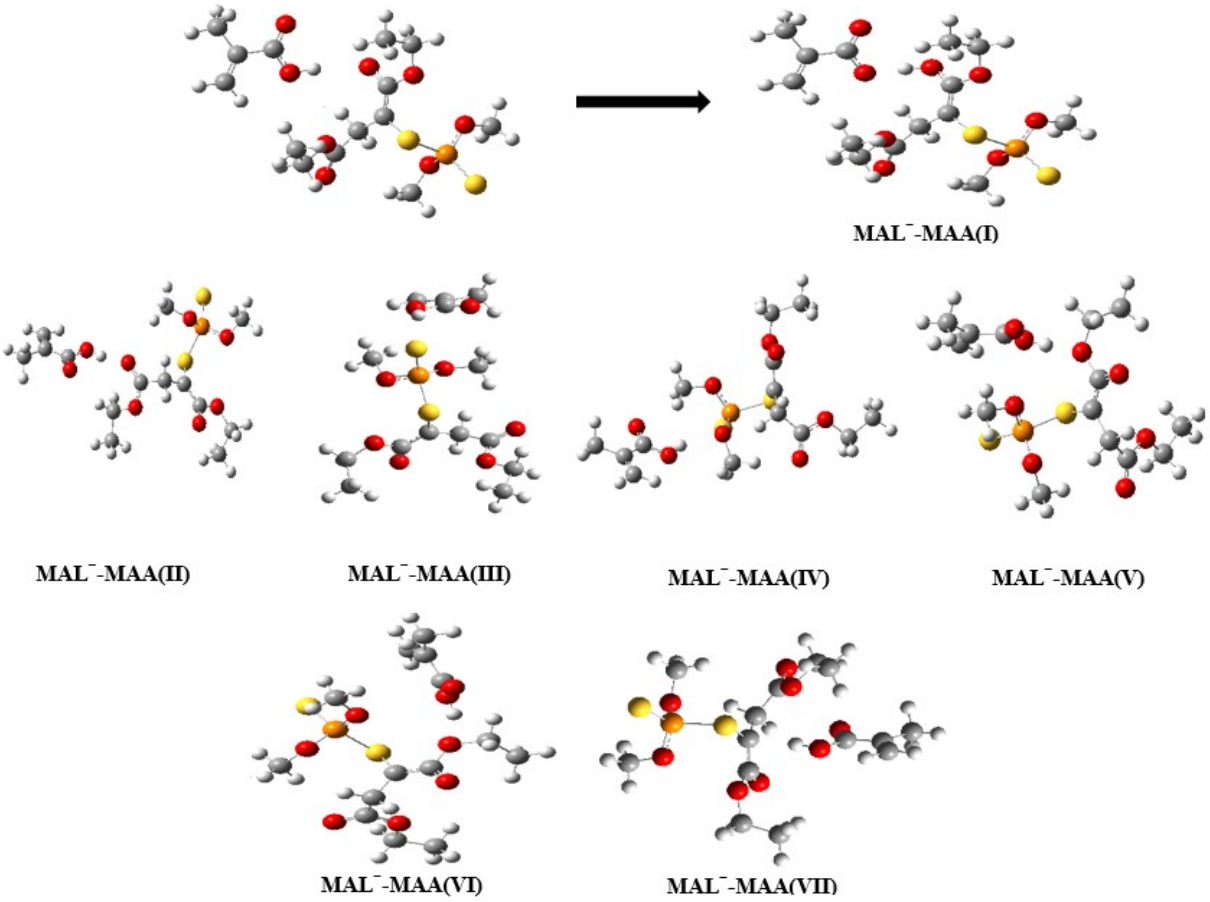
MAL¯-MAA(I)
MAL¯-MAA(II)
MAL¯-MAA(III)
MAL¯-MAA(IV)
MAL¯-MAA(V)
MAL¯-MAA(VI)
MAL¯-MAA(VII)

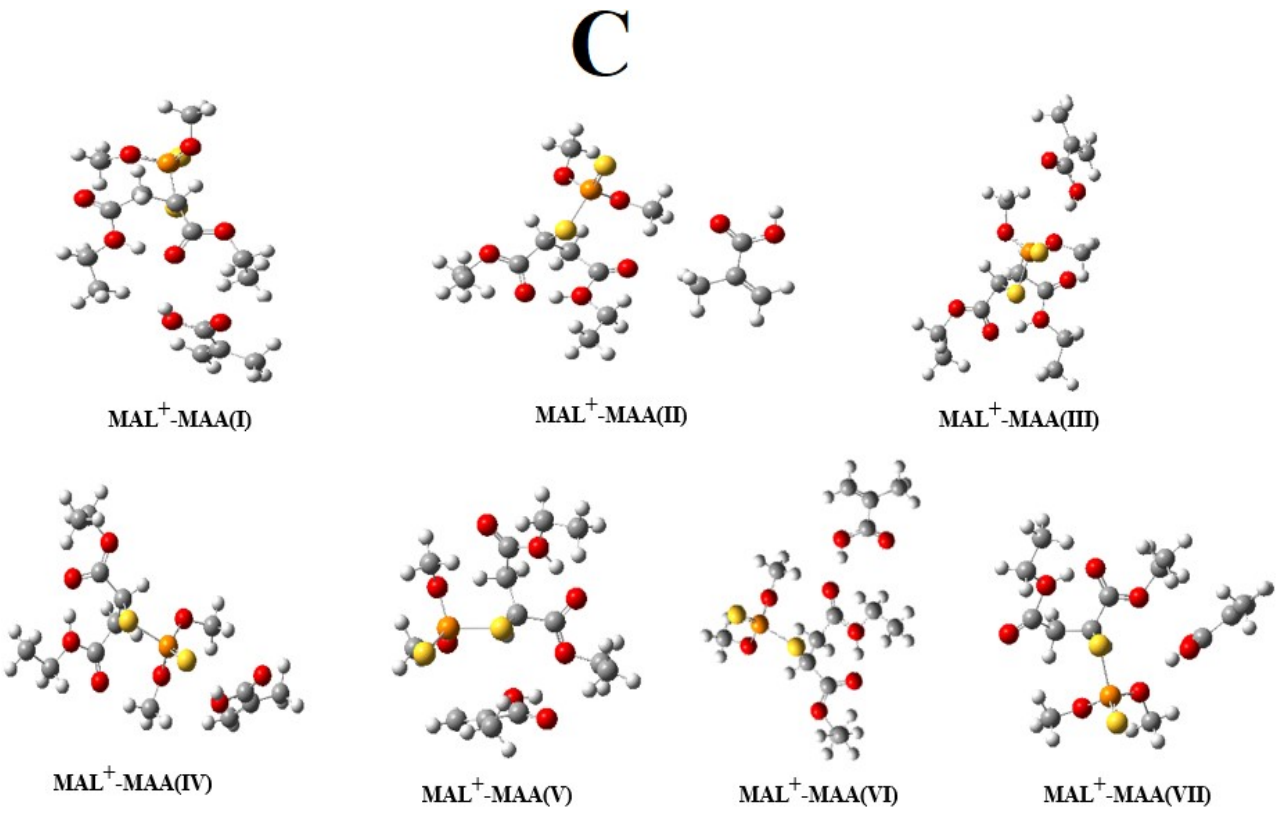

Figure 11S. (A) the optimized forms of MAL–MAA complexes in neutral media, (B) the optimized forms of MAl^{-}–MAA complexes in alkaline media, (C) the optimized form of MAl^{+}–MAA complex in acidic media.

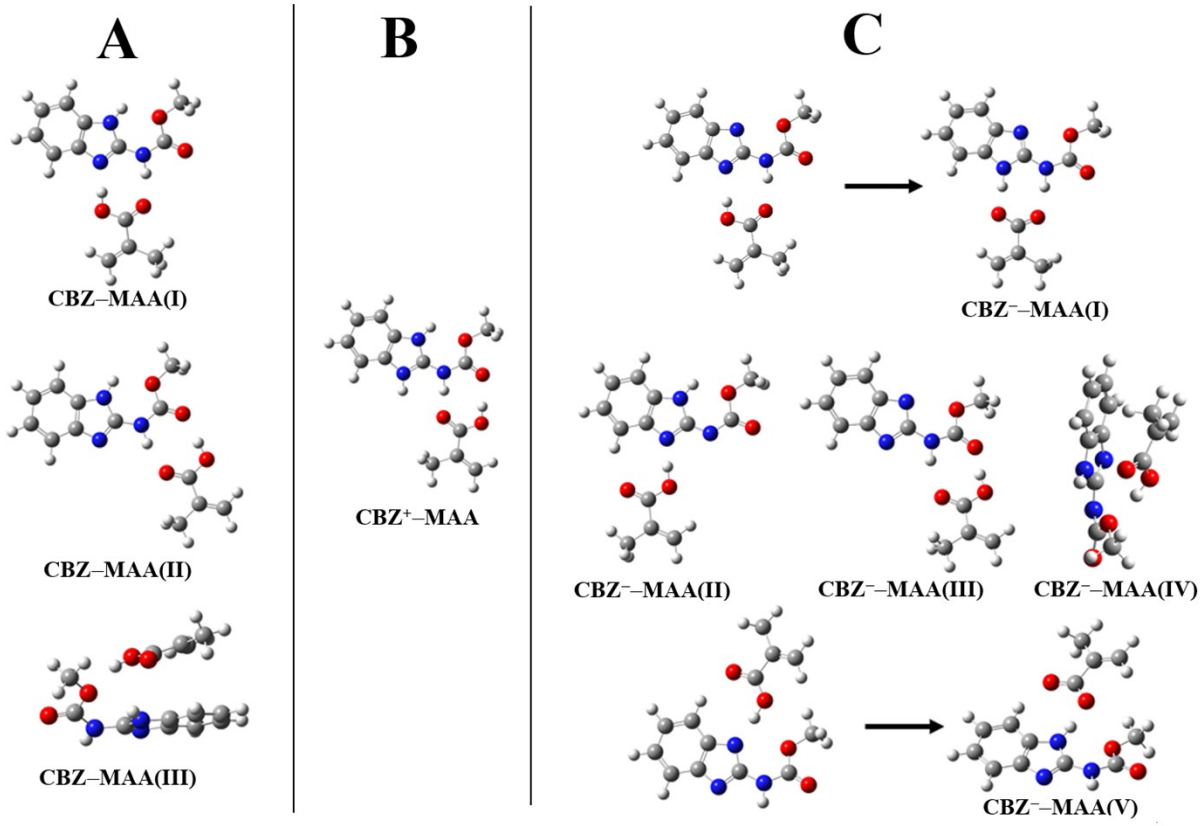

Figure 12S. (A) The optimized forms of CBZ–MAA complexes in neutral media, (B**)** the optimized form of CBZ^{+}–MAA complex in acidic media, (C) the optimized forms of CBZ^{-}–MAA complexes in alkaline media.

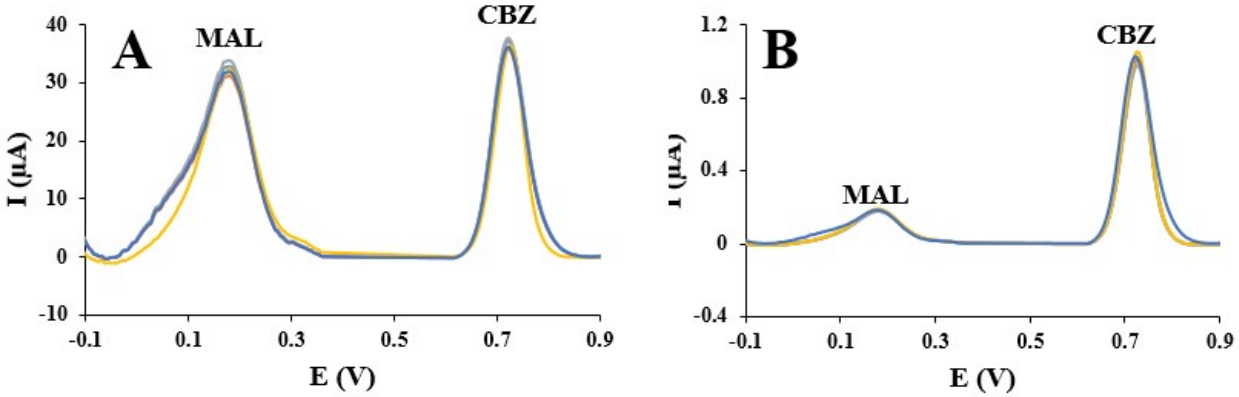

Figure 13S. (A) DPV curves of the GQDs@MIP-GECE in 0.1M PBS (pH 7.0) after rebinding 32.0 µM MAL and 22.0 µM CBZ (A), and after rebinding 0.1 µM MAL and 0.5 µM CBZ (B), in the range potential of -0.1 to 0.9 V with five repetitions.